Journal of Medical Devices Technology Vol. 2, No. 2, (2023) 72-78

Journal of Medical Devices Technology

jmeditec.utm.my

Original Research

Reduced-Size Antenna for Leadless Cardiac Pacemaker

DiviyaDevi Paramasivam[1,2], Raimi Dewan[1,2, 3*], Nuradilah Yusri[1,2]

[1] *Advanced Radio Frequency & Microwave Research Group, Faculty of Electrical Engineering, Universiti Teknologi Malaysia, 81310 UTM Johor Bahru, Malaysia*
[2] *IJN-UTM Cardiovascular Engineering Centre, Institute of Human Centered Engineering, Universiti Teknologi Malaysia, 81310 UTM Johor Bahru, Malaysia.*
[3] *Department of Biomedical Engineering and Health Sciences, Faculty of Electrical Engineering, Universiti Teknologi Malaysia, 81310 UTM Johor Bahru, Malaysia*

ARTICLE INFO

Article History:
Received 16 August 2023
Accepted 22 November 2023
Available online 20 December 2023

Keywords:
Antenna,
Implantable,
LCP,
Reduced-size

ABSTRACT

The advancement in technology led to the development of leadless cardiac pacemaker (LCP) systems that resolved the issues that arise due to the use of leads in the conventional pacemakers (CP). However, the compact size of the LCP system also requires a miniaturized antenna that can fit inside the limited space of the LCP. Therefore, this study was conducted to propose and design a reduced-size antenna that operates at 2.4 GHz. An implantable antenna with a footprint of 4.00 × 5.00 × 0.50 mm was designed using CST Microwave Studio (student version). An LCP system was integrated with the antenna and simulated inside the heart tissue model to evaluate the performance of the antenna. Based on the S_{11} parameter, the antenna was further optimized, and the coaxial-feed cable position was offset until the impedance matching was achieved for the resonant frequency to be at 2.4 GHz. The antenna exhibited good performance with a S_{11} of less than -10 dB at 2.4 GHz. In addition, the proposed antenna satisfies the requirements of LCP with limited space. Therefore, the proposed antenna is envisaged to be implemented for LCP systems.

INTRODUCTION

A pacemaker is a small, battery-powered implantable medical device (IMD) that is used to monitor and regulate the heartbeat of people with a slow or irregular heart rate. According to Market Research Future, it is anticipated that, by 2030, the global market for pacemakers will reach USD 6.6 billion (Market Research Future, 2023). The increment in the number of cases of cardiovascular diseases and the growing geriatric population are the reasons behind the growth.

A typical conventional pacemaker (CP) is comprised of three main components, such as a pulse generator, two leads, and electrodes that are made of biocompatible materials (Merchant & Mittal, 2020). CP is implanted under the chest's skin, and the leads are implanted inside the veins that lead to the heart (Yi et al., 2022). The pulse generator produces the electrical current that is required to stimulate the heart muscle while the leads transmit the electric current to the heart muscles (Lak & Goyal, 2022). For instance, if the heart rate is slower than normal, an electrical impulse will be sent through the lead to the electrode. As a result, the heart begins to beat fast, and the normal heartbeat rhythm will be achieved (Pacemaker insertion, 2021). Although CP is able to regulate the heart rate, several issues are raised. The major problem that remained unsolved is the infection caused by the implantation, which even cost lives. According to recent research, it has been found that every 14th patient undergoing CP implantation was affected by infection, and among them, every 5th led to death (Asif et al., 2019). Not only that, the implantation of the leads causes the central vein to obstruct, pneumothorax and tricuspid failure (Sharma et al., 2022). Therefore, leadless pacemakers, or leadless cardiac pacemakers (LCP), were introduced by St. Jude Medical and Medtronic to overcome the shortcomings related to the CP. They

* Raimi Dewan (raimi.dar@utm.my)
Department of Biomedical Engineering & Health Sciences Department, Faculty of Electrical Engineering, Universiti Teknologi Malaysia, 81310 UTM Johor Bahru, Johor, Malaysia.

developed LCP systems such as Nanostim LCP and Micra transcatheter pacing systems (TPS) (Zada et al., 2021).

LCP is a capsule-like device that consists of several components, as shown in Figure 1. When comparing the LCP with the CP, LCP has a pulse generator and electrode in a single unit, which eliminates the need for leads (Sharma et al., 2022). In addition, LCP will be directly implanted in the right ventricle of the heart. Moreover, the LCP has a smaller dimension compared to the CP (Sharma et al., 2022). Besides this, the LCP implantation procedure is less invasive because a chest incision is not required as in CP, and it will not form a scar or bump under the skin (Medtronic. (n.d.); Zada et al., 2021). Despite these advantages, there are some limitations associated with LCP, such as battery longevity, efficacy, and wireless telemetry (Sharma et al., 2022; Zada et al., 2021).

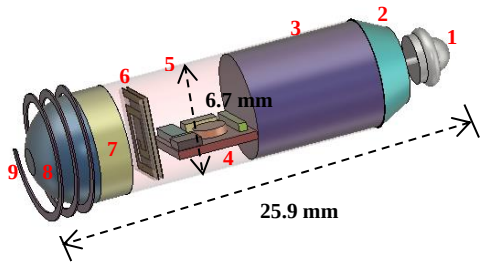

Components of LCP:
1. Docking button
2. Lid
3. Battery
4. PCB
5. Container
6. Antenna
7. Circuit Holder
8. Electrode
9. Helix

Fig. 1 Schematic diagram of the LCP and its components.

Among these limitations, biotelemetry is one of the most crucial aspects of active IMD. This is because it allows communication between the antennas of the IMD and the external patient monitoring devices' antennas to enable medical personnel to monitor the heart rate of patients (Zada et al., 2021). Therefore, it is important to take into account several factors before developing an antenna for the LCP systems. One of the factors that need to be considered is the space available for the antenna inside the IMD devices. This is because the development of ultra-small IMD devices such as Nanostim and Micra TPS has limited space for the accommodation of the antenna (Zada et al., 2021).

Recently, researchers have focused on developing miniaturized antennas for LCP systems. A conformal antenna that wrapped around the dummy pacemaker was proposed by Asif et al. (2019) with a dimension of 17.28 × 14.28 × 0.29 mm^3. The antenna was operated in the Industrial, Scientific, and Medical (ISM) band of 2.45 GHz with a peak gain of -35 dBi. Similarly, a conformal antenna was proposed by Bose et al. (2019) with a dimension of 10.00 mm × 9.00 mm. The antenna worked at 433 MHz, which is in the ISM band. From the studies above, the antennas are compact in structure. However, the integration of the conformal antennas with the circuitry system of the LCP is difficult (Zada et al., 2021).

Sha et al. (2019) proposed a flat antenna with a dimension of 7.00 mm × 6.50 mm × 0.38 mm that worked at multiple frequency bands for LCP systems. Similarly, Ramzan et al. (2019) also proposed a spiral antenna with a radius of 5 mm and operating at 402-405 MHz, which is a Medical Implant Communication Service (MICS) band. Although these antennas' are compact in size and are developed for LCP systems, they are not compatible in terms of size with the commercially available LCP systems such as the Nanostim and Micra TPS which has a dimension of 5.99 mm × 42.00 mm and 6.70 mm × 25.90 mm, respectively (Beurskens et al., 2017). Therefore, a reduced-size antenna that can fit inside the LCP systems is preferred.

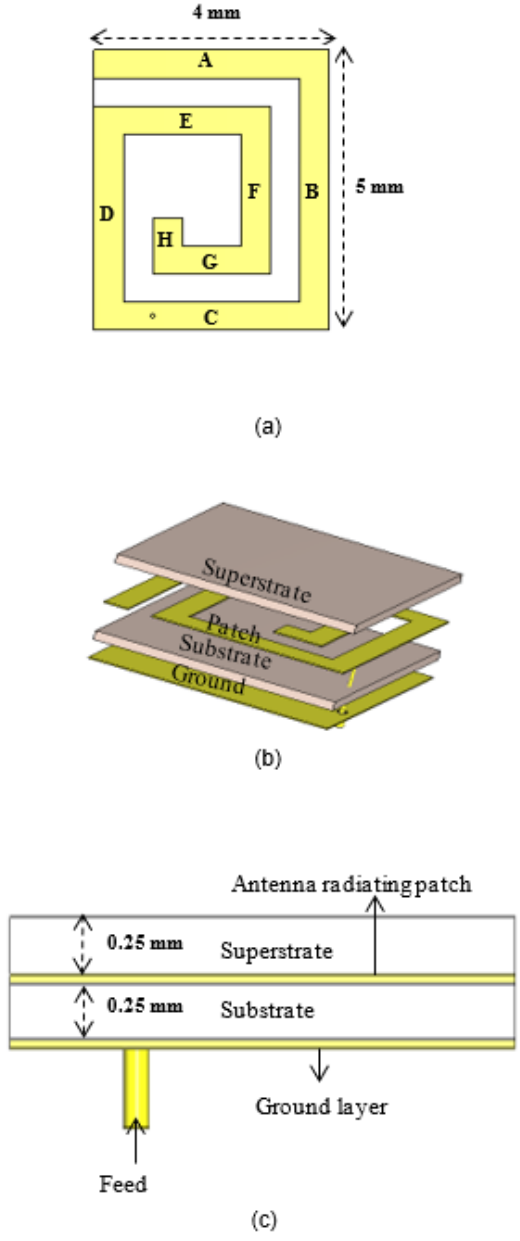

Fig. 2 Detailed structure of the proposed antenna in (a) front view (b) exploded view (c) side view.

In this study, a reduced-size implantable antenna with a footprint of 4.00 × 5.00 × 0.50 mm was proposed and simulated with the LCP system in a heart model using CST Microwave Studio. The size reduction is achieved using the squared spiral-shaped radiating patch, substrate, and superstrate with high dielectric properties.

METHODOLOGY

Figure 2 shows the configuration of the pre-optimized antenna. The antenna has a squared spiral-shaped radiating patch, which eases the fabrication process. In addition, it is also found that the body's dielectric variations are less likely to affect the spiral-shaped antennas as they are less sensitive to the dielectric variations (Kim & Shin, 2019). Therefore, a reduced-sized squared spiral-shaped antenna that operates at the ISM band of 2.4 GHz with a footprint of 4.00 × 5.00 × 0.50 mm was designed, simulated, and optimized using CST Microwave Studio. The antenna designing was started by approximating the size of the antenna, which was half the value of effective operating wavelength ($\lambda/2$). Then, the antenna size was reduced until it fits inside the LCP system. Table 1 shows the dimensions used for the length and width of radiating patch.

Table 1 Dimensions of the proposed antenna

Element	Value (mm)	Description
LA	4.00	Length
WA	0.50	Width
LB	5.00	Length
WB	0.50	Width
LC	4.00	Length
WC	0.50	Width
LD	4.00	Length
WD	0.50	Width
LE	3.00	Length
WE	0.50	Width
LF	3.00	Length
WF	0.50	Width
LG	2.00	Length
WG	0.50	Width
LH	1.00	Length
WH	0.50	Width

The proposed antenna's radiating patch was made up of copper with a thickness of 0.035 mm, and for the substrate, Rogers RT/Duroid 3010 with a thickness of 0.25 mm, permittivity of 10.20, and a loss tangent of 0.0023 was used (Singh & Kaur, 2021; Salama et al., 2020). The high permittivity of the Rogers RT/Duroid 3010 enables the miniaturization of the antenna by decreasing the antenna losses and reducing the effective wavelength (Feng et al., 2022). Based on these advantages, the Rogers RT/Duroid 3010 was selected to be used as the substrate. In addition, a superstrate layer made up of Rogers RT/Duroid 3010 with a dimension similar to the substrate was used because it serves as the insulation layer. (Feng et al., 2022). Lastly, the proposed antenna was fed with a flexible coaxial cable.

Pre-optimization of the Proposed Antenna

Four design iterations were carried out in the pre-optimisation stage, as shown in Figure 3. In each iteration the number of sides with different lengths and similar widths (0.5 mm) was added one by one, as illustrated in Figure 3. The addition of the sides was continued until the operating frequency resonates at 2.4 GHz. The design of the proposed antenna began with a one square loop as presented in iteration 1. In iteration 2, a side with a length (LF) of 3 mm was added. In iteration 3, a side with a length (LE) of 2 mm was added, as shown in Figure 3(c). Lastly, a short side with a length (LF) of 1 mm was added. All the iterations were carried out with the excitation position at X = 1.00 and Y = 0.25, as shown in Figure 4. This position was selected by trial-and-error method by choosing a distance of 50.00% from the below and 25% from the edge. The chosen position provides maximum impedance matching.

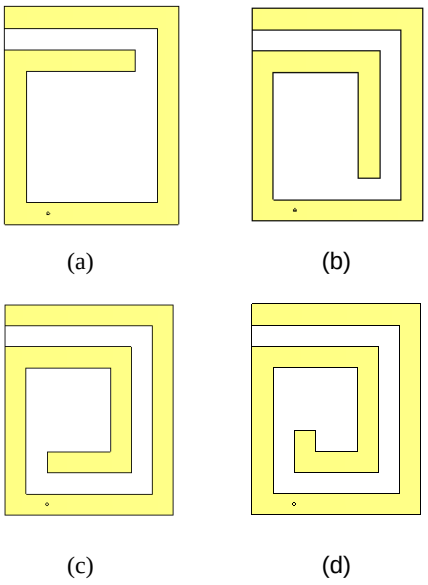

Fig. 3 Proposed antenna's design evolution (a) iteration 1 (b) iteration 2 (c) iteration 3 (d) iteration 4.

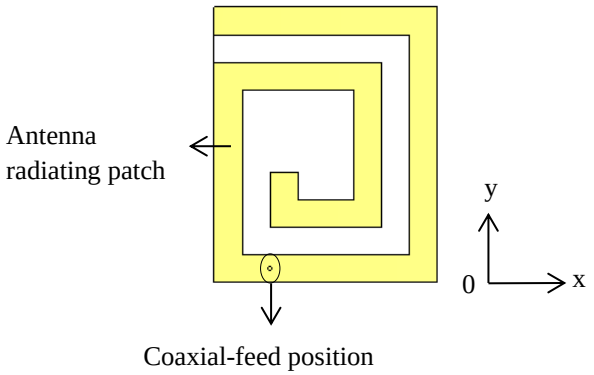

Fig. 4 Excitation position of the antenna

Integrating Proposed Antenna with LCP

A LCP with standard dimensions of 25.90 mm × 6.70 mm was designed using CST Microwave Studio student version and integrated with the proposed antenna. For the simulation, the components of the LCP, such as the battery, helix, electrode, and circuitry, are set as perfect electric conductors (PEC). In addition, polylactic acid (PLA) with a permittivity of 3.1094 and a loss tangent of 0.0053 was used to enclose all the elements (Linge et al., 2023). The use of PLA provides biocompatibility, which will prevent the rejection of the LCP when it is implanted (Das et al., 2022; Tesser et al., 2019). After the integration, the simulation was carried out to determine the performance of the antenna inside the LCP.

Simulation of Implantation of LCP Integrated with the Proposed Antenna

The LCP integrated with the proposed antenna was placed centered of the human heart tissue model with dimensions, as shown in Figure 5. The permittivity of 54.918 and conductivity of 2.215 S/m were used for the heart tissue model because these dielectric properties are for the operating frequency range of 1.8 to 3 GHz (Feng et al., 2022; Zada et al., 2021). The simulation was carried out, and the S_{11} parameter was obtained. The antenna dimension was optimized in terms of the length and width of the radiating patch until the resonant frequency was 2.4 GHz. The appropriate dimension of the radiating patch was obtained after eight iterations. Similarly, the position of the coaxial-feed was also adjusted by performing twelve iterations until maximum impedance matching was obtained.

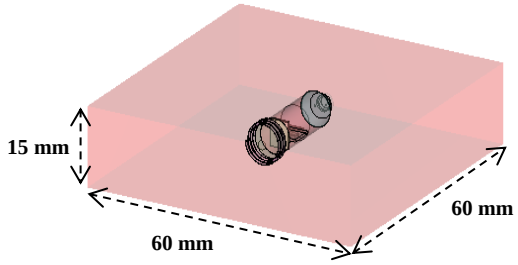

Fig. 5 Simulation of LCP integrated with proposed antenna.

RESULTS AND DISCUSSION

In this paper, the S_{11} parameter of the antenna was obtained by optimizing the dimensions of the radiating patch of the antenna and adjusting the coaxial-feed position.

Pre-optimization of the Proposed Antenna

In iteration 1, the resonant frequency was 3.05 GHz, which is not at the desired ISM band (2.4 GHz). In addition, the S_{11} of the antenna was -4.31 dB, which was more than -10 dB, as illustrated in Figure 6. To shift the resonant frequency to the left, side F was added in iteration 2. The addition of side F causes the resonant frequency to shift left, as it was observed at 2.63 GHz. However, the S_{11} further increases to -0.23 dB. The increase in the S_{11} showed that the power loss is greater than the power radiated by the antenna.

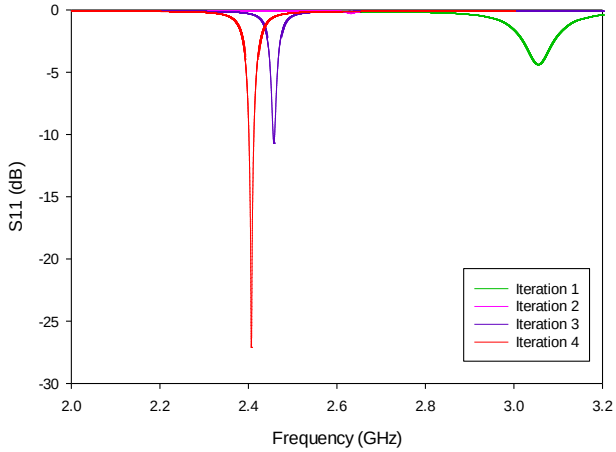

Fig. 6 S_{11} parameter comparison between antenna with different iterations.

Therefore, iteration 3 was carried out by adding side G. In iteration 3, the resonant frequency was 2.45 MHz which is within the ISM band, with a S_{11} of -10.66 dB. Since the desired operating frequency is 2.4 GHz, iteration 4 was carried out, where it was able to resonate at 2.4 GHz with a S_{11} of -25.73 dB, which was less than the one in iteration 3. This showed that the antenna in iteration 4 was able to radiate almost all the power with little power loss compared to other iterations. Therefore, the antenna proposed in iteration 4 was used for the rest of the study. It is worth noting that the iterations improved the performance of the antenna.

Simulation of Proposed Antenna with LCP

The S_{11} parameter of the LCP integrated with the antenna shows that the proposed antenna satisfies the condition, where it resonates at 2.4 GHz and has a S_{11} of -27.96 dB, which is lower than -10 dB, as shown in Figure 7. Therefore, the LCP integrated with the proposed antenna, simulated inside a heart tissue to determine the performance of the antenna in a high permittivity medium.

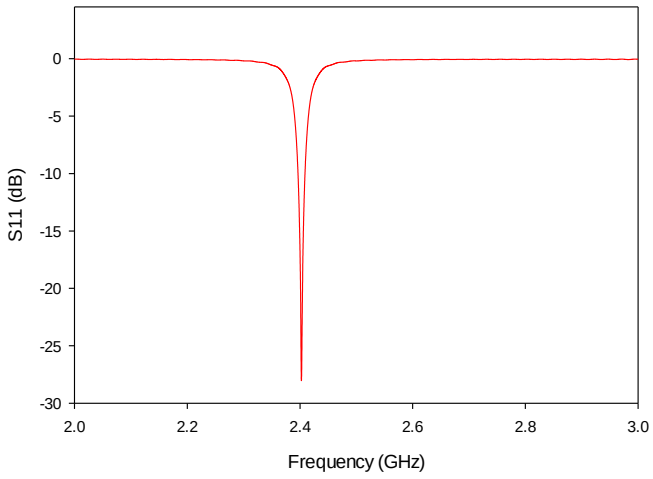

Fig. 7 S_{11} parameter of LCP integrated with antenna.

Simulation of Implantation of LCP Integrated with the Proposed Antenna

The LCP integrated with the proposed antenna simulated inside the heart tissue model. Based on Figure 8, it can be seen that the resonant frequency was shifted right from 2.4 GHz to 3.19 GHz with a S_{11} of -12.64 dB. This is due to the high permittivity of the tissue, which causes the resonant frequency to shift (Suryanata et al., 2023). Therefore, optimization was carried out to shift the resonant frequency, as shown in Figure 8. The optimization was carried out by reducing and increasing the dimensions of the radiating patch alternately. After eighth iteration, of changing the length and width of the radiating patch as tabulated in Table 2, the resonant frequency shifted to 2.33 GHz with a S_{11} of -3.53 dB. Since the resonance frequency is not at 2.4 GHz, the coaxial-feed position was adjusted.

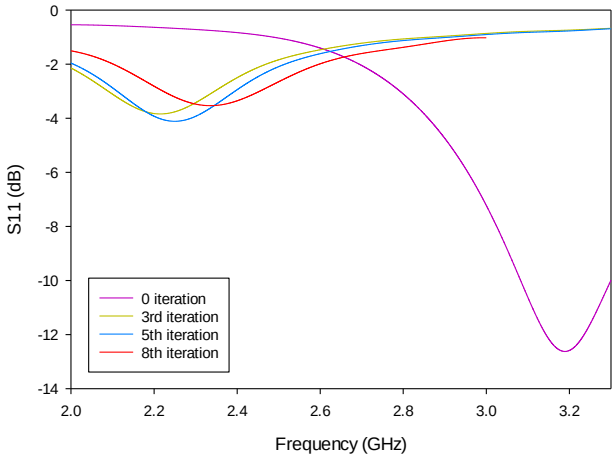

Fig. 8 S_{11} parameter of LCP integrated with antenna in heart tissue model with different iterations

Table 2 Parameter iteration for second stage optimization of antenna

Element	Parameter iterations			Description
	3rd	5th	8th	
LA	4.00	4.00	4.00	Length
WA	1.00	1.00	0.50	Width
LB	5.00	5.00	5.00	Length
WB	1.00	1.00	1.00	Width
LC	4.00	4.00	4.00	Length
WC	1.00	1.00	1.00	Width
LD	3.50	3.50	3.50	Length
WD	1.00	1.00	1.00	Width
LE	2.50	2.50	2.50	Length
WE	0.50	0.50	0.75	Width
LF	2.00	2.00	2.00	Length
WF	0.50	0.50	0.25	Width
LG	1.00	1.00	1.00	Length
WG	0.50	0.50	0.25	Width
LH	0.63	0.63	0.63	Length
WH	0.25	0.25	0.25	Width

Based on Figure 9, it can be seen that adjusting the coaxial-feed position shifts the resonant frequency and also improves the S_{11} value. In first iteration, the X position was maintained while the Y position was changed from 0.25 to 3.35. This adjustment causes the resonant frequency to shift from 2.33 GHz to 2.34 GHz, and the S_{11} was decreased to -12.49 dB. To further improve, the X position was increased to 1.25 while the Y position was maintained at 3.35, as shown in Table 3. The S_{11} was decreased to -13.85 dB, but the resonant frequency was maintained at 2.34 GHz. Next, the iterations were carried out by further increasing the X position by 0.50. A slight shift was observed for the resonant frequency (2.35 GHz), and the S_{11} was -15.31 dB. The adjustment was continued by increasing the X position and decreasing the Y position, as shown in Table 3. In eleventh iteration, the resonant frequency was shifted right to 2.38 GHz, and the S_{11} was decreased to -20.85 dB. Finally, during the twelfth iteration, the resonant frequency was shifted to 2.4GHz, and the S_{11} was decreased to -22.45 dB, as shown in Figure 9. This shows that adjusting the excitation position will improve the performance of the antenna as it provides better impedance matching.

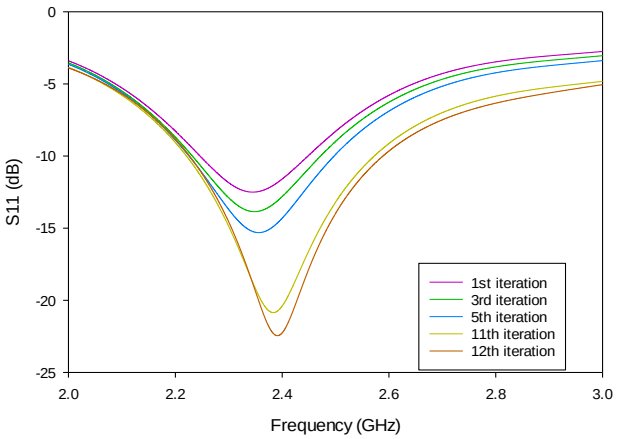

Fig.9 S_{11} parameter of antenna with different excitation positions

Table 3 Parameter iteration for coaxial-feed position.

Element	Iterations				
	1st	3rd	5th	11th	12th
X	1.00	1.50	2.00	2.35	2.38
Y	3.35	3.35	3.35	2.00	1.70

The proposed antenna was compared with the antennas reported in the literature for the LCP systems, as shown in Table 4. The proposed antenna achieved a 71.43 to 90.00% size reduction and realized gain difference of -1.96 to 13.34 dBi. Therefore, the proposed antenna successfully reduced the size by 70.43 to 90.00% and realized gain difference of 13.34 dBi.

Table 4 Comparison of size and realized gain of proposed antenna with previous work

Ref.	Volume (mm^3)	Size in λ_r (mm^3)	Size reduction (%)	Realized gain (dBi)	Realized gain difference (dBi)
(Asif et al., 2019)	17.28 × 14.28 × 0.29	0.58	86.21	-35.00	13.34
(Ketavath et al., 2019)	24.00 × 22.00 × 0.07	0.30	73.33	-19.70	-1.96
(Wang et al., 2021)	12.00 × 12.00 × 0.64	0.28	71.43	-34.00	12.34
(Xia et al., 2020)	9.80 × 9.80 × 1.27	0.98	90.00	-33.00	11.34
Proposed work	4.00 × 5.00 × 0.50	0.08	-	-21.66	-

CONCLUSION

A reduced-size antenna for LCP systems was designed and optimized. The proposed antenna's performance was simulated by integrating the antenna with LCP and inside heart tissue model. The optimization of the antenna was carried out inside the heart tissue model by altering the dimensions of the length and width of the radiating patch of the antenna and also by adjusting the coaxial-fed position. The proposed antenna achieved a 90.00% reduction in size and realized gain difference of 13.34 dBi when compared with the reported antenna for LCP systems. Therefore, this antenna satisfies the requirements of LCP systems, such as compact size with acceptable performance. The reduced size of antenna would open up the possibility to further reduced size of the entire LCP.

ACKNOWLEDGMENT

The authors would like to thank the Ministry of Higher Education (MOHE), School of Postgraduate Studies (SPS), Research Management Centre, Advanced RF and Microwave research group, IJN-UTM Cardiovascular Engineering Centre and Universiti Teknologi Malaysia (UTM), Johor Bahru, for the support of the research under Fundamental Research Grant Scheme R.J130000.7823.5F678 and UTM Encouragement Research Grant Q.J130000.3851.20J74.

REFERENCES

Asif, S. M., Iftikhar, A., Braaten, B. D., Ewert, D. L., Maile, K. 2019. A wide-band tissue numerical model for deeply implantable ntennas for RF-powered leadless pacemakers. IEEE Access: Practical Innovations, Open Solutions, 7.

Beurskens, N. E., Tjong, F. V., Knops, R. E. 2017. End-of-life management of leadless cardiac pacemaker therapy. Arrhythmia & Electrophysiology Review, 6(3), 129–133.

Bose, P., Khaleghi, A., Mahmood, S., Albatat, M., Bergsland, J., Balasingham, I. 2019. Evaluation of data telemetry for future leadless cardiac pacemaker. IEEE Access: Practical Innovations, Open Solutions, 7, 157933–157945.

Das, S., Mitra, D., Chezhian, A. S., Mandal, B., Augustine, R. 2022. A novel SAR reduction technique for implantable antenna using conformal absorber metasurface. Frontiers in Medical Technology, 4.

Feng, Y., Li, Z., Qi, L., Shen, W., & Li, G. 2022. A compact and miniaturized implantable antenna for ISM band in wireless cardiac pacemaker system. Scientific Reports, 12(1), 1–11.

Ketavath, K. N., Gopi, D., Sandhya Rani, S. 2019. In-vitro test of miniaturized CPW-fed implantable conformal patch antenna at ISM band for biomedical applications. IEEE Access: Practical Innovations, Open Solutions, 7, 43547–43554.

Kim, S., Shin, H. 2019. An ultra-wideband conformal meandered loop antenna for wireless capsule endoscopy. Journal of Electromagnetic Engineering and Science, 19(2), 101–106.

Lak, H. M., Goyal, A. 2022. Pacemaker Types and Selection. StatPearls Publishing.

Linge, P. U., Gerges, T., Bevilacqua, P., Duchamp, J.-M., Benech, P., Verdier, J., Lombard, P., Cabrera, M., Tsafack, P., Mieyeville, F., Allard, B. 2023. Evaluation of polylactic acid polymer as a substrate in rectenna for ambient radiofrequency energy harvesting. Journal of Low Power Electronics and Applications, 13(2), 34.

Market Research Future. (2023, June 13). Pacemaker market size to surpass USD 4.2 billion by 2030 at 3.60% CAGR – report by market research future (MRFR). Market Research Future. https://www.globenewswire.com/news-release/2023/06/13/2687705/0/en/Pacemaker-Market-Size-to-Surpass-USD-4-2-Billion-by-2030-at-3-60-CAGR-Report-by-Market-Research-Future-MRFR.html

Medtronic. (n.d.). Micra - pacemakers. Medtronic.com. Retrieved August 4, 2023, from https://www.medtronic.com/us-en/patients/treatments-therapies/pacemakers/our/micra.html

Merchant, F. M., Mittal, S. 2020. Pacing induced cardiomyopathy. Journal of Cardiovascular Electrophysiology, 31(1), 286–292.

Pacemaker insertion. (2021, August 8). Hopkinsmedicine.org. https://www.hopkinsmedicine.org/health/treatment-tests-and-therapies/pacemaker-insertion

Ramzan, M., Fang, X., Wang, Q., Neumann, N., Plettemeier, D. 2019. Miniaturized planar implanted spiral antenna inside the heart muscle at MICS band for future leadless pacemakers. 13th International Symposium on Medical Information and Communication Technology (ISMICT), 1–4.

Salama, S., Zyoud, D., Daghlas, R., Abuelhaija, A. 2020. Design of a planar inverted F-antenna for medical implant communications services band. Journal of Physics. Conference Series, 1711(1), 012001.

Shah, I. A., Zada, M., Yoo, H. 2019. Design and analysis of a compact-sized multiband spiral-shaped implantable antenna for scalp implantable and leadless pacemaker systems. IEEE Transactions on Antennas and Propagation, 67(6), 4230–4234.

Sharma, D., Kanaujia, B. K., Kaim, V., Mittra, R., Arya, R. K., Matekovits, L. 2022. Design and implementation of compact dual-band conformal antenna for leadless cardiac pacemaker system. Scientific Reports, 12(1), 3165.

Singh, G., Kaur, J. 2021. In-silico and in-vitro testing of an implantable superstrate loaded biocompatible antenna for MICS band applications. Microwave and Optical Technology Letters, 63(3), 910–916.

Suryanata, F. A., Muhammad, N. F., Azizi, N. N. A., Dewan, R., Roy, B. 2023. Performance analysis of wearable antenna worn in close proximity with human body. Journal of Medical Device Technology, 2(1), 43–49.

Tesser, A., Alemaryeen, A., Lewis, J., Alshami, A., Haghshenas, M., Noghanian, S. 2019. Synthesis and use of bio-based dielectric substrate for implanted radio frequency antennas. IEEE Access: Practical Innovations, Open Solutions, 7, 123268–123279.

Wang, M., Liu, H., Zhang, P., Zhang, X., Yang, H., Zhou, G., Li, L. 2021. Broadband implantable antenna for wireless power transfer in cardiac pacemaker applications. IEEE Journal of Electromagnetics, RF and Microwaves in Medicine and Biology, 5(1), 2–8.

Xia, Z., Li, H., Lee, Z., Xiao, S., Shao, W., Ding, X., & Yang, X. 2020. A wideband circularly polarized implantable patch antenna for ISM band biomedical applications. IEEE Transactions on Antennas and Propagation, 68(3), 2399–2404.

Yi, Y., Huang, T., Xu, Y., Mei, J., Zhang, Y., Wang, X., Chen, J., Ying, G. 2022. Preparation and properties of N-glycosylated chitosan/polyvinyl alcohol hydrogels for use in wound dressings. Journal of Applied Biomaterials & Functional.

Zada, M., Shah, I. A., Basir, A., Yoo, H. 2021. Ultra-compact implantable antenna with enhanced performance for leadless cardiac pacemaker system. IEEE Transactions on Antennas and Propagation, 69(2), 1152–1157.